Available online at www.sciencedirect.com

SciVerse ScienceDirect

Procedia Engineering 58 (2013) 418 – 423

Procedia Engineering

www.elsevier.com/locate/procedia

The 12th Hypervelocity Impact Symposium

Investigations of rf Emissions from Hypervelocity Impacts of Various Metals

William. T. Brown [a]*, Mark. F. Schmidt[b] and William Broad[b]

[a]*Applied Research Associates Inc, Arlington, VA 22203, USA*

[b]*Applied Research Associates Inc, Littleton, CO 80127,USA*

Abstract

We describe a series of experiments to examine emissions in the radio-frequency (RF) portion of the electromagnetic spectrum, resulting from hyper-velocity impacts of various metals. A two-stage gas gun was used to impact aluminium (6061-T6) spheres, at velocities of approximately 6 km/s and 9 km/s, against aluminium/titanium alloy (Ti6Al4v) target plates. In most experiments, debris ejected from the rear surfaces of target plates impacted against witness plates of various metals (aluminium, copper, zinc, etc). The witness plates were placed at various distances from rear surfaces of target plates, and electric field probes were used to obtain measurements of three near-field orthogonal components of the electric fields at sampling rates of 10 giga-samples/s. From experimental and computational results, we have developed a semi-empirical model describing dependence of the electric field amplitude and frequency on material strength and impact conditions.

Selection and peer-review under responsibility of the Hypervelocity Impact Society

Keywords: Hypervelocity Impact; Electromagnetic Emissions; OREX; Fragmentation l

Nomenclature

E_i	vector components of the electric field (V/m)
U	electromagnetic energy density (J/m^3)
Δt	time duration of a discrete EM pulse (s)
ε_0	permittivy of free space (F/m)

1. Introduction

We have executed a series of gas gun impact experiments to determine spectral and temporal characteristics of RF emissions generated by impacts of various metals of interest. These experiments were performed at Sandia National Laboratories (SNL), jointly with personnel from the Naval Research Laboratory (NRL), Corvid, Inc and Prism, Inc; they collected data in other portions of the electromagnetic spectrum that are reported separately. We used the acronym OREX to describe these **O**ptical and **R**F **E**mission **E**xperiments. To aid our understanding of the physical and thermodynamic

* Corresponding author. Tel.: +1 703-816-8886; fax: +1 000-000-0000.
E-mail address: wbrown@ara.com.

Selection and peer-review under responsibility of the Hypervelocity Impact Society
doi:10.1016/j.proeng.2013.05.048

environments of the impact experiments, we modelled the events using finite-difference methods. In our data analysis process, we attempted to develop correlations between material physical properties and measured RF emissions.

2. Background

In prior research efforts, we have investigated electromagnetic emissions resulting from the detonation of metal-encased explosives; this research has shown that such emissions are caused primarily by high strain-rate fracture of metals [1 - 4]. We demonstrated that [3] the electromagnetic emissions resulting from the detonation of metal encased explosives can be characterized in terms of several parameters that are used to quantify generation of fragments during the rupture of cylinder containing the explosives. Furthermore, we found that impact experiments could be designed in a manner that allowed us to approximate the facture conditions occurring during explosions. This made it possible for us to develop a method for analyzing electromagnetic emissions using a stochastic approach. We concluded that the distribution function describing the statistics of fragment size can be used to deduce the distribution of amplitudes and frequencies of the electromagnetic emissions, or vice versa.

3. Description of experiments

In the OREX events, we used projectiles at velocities of approximately 6 km/s to observe RF emissions from various metal targets. In most of these events, 6.35mm diameter aluminum spheres were impacted against target plates of aluminum/titanium alloys, and a witness plate was placed 200mm behind the target plate. Various materials were used as witness plates. In some of the events, a second witness plate was placed behind the primary witness plate. The configurations used during OREX-1 through OREX-7 are listed in the table below. We collected RF data on multiple channels at a rate of 10 Giga-sample/s during a total time of 4.8ms. Additional experiments were performed at approximately 9 km/s; they are not discussed in this paper.

The three-stage light gas gun at the SNL **S**hock **T**hermodynamics and **A**pplied **R**esearch (STAR) facility was used to launch aluminum spherical projectiles (6.35mm diameter) to velocities of approximately 6 km/s. The system uses a Lexan sabot to allow for acceleration of the projectile; the sabot is stripped away prior to impact of the projectile again the target plate. During a period of free-flight, prior to impact, the impactor passes through the Magnetic Velocity Induction System (MAVIS) that provides a very accurate determination of impact velocity [5].

Fig. 1.Configuration of the trio of E-field probes used to measure impact-generated RF emissions. The red arrow shows the exit point of the impactor from the launch section into the impact chamber.

A trigger system was used to activate the data collection system several microseconds prior to projectile impact. Electric field probes, as shown in Figures 1, were placed in the impact chamber, and used to measure electric field emissions from the target plates and witness plates. Because the probes where in the near-field of the emitting source, we measured three vector components of the electric field, and found the radial component to be stronger than the transverse components. We also placed a triad of probe outside of the impact chamber. Our instrumentation included a trio of E-field sensors to collect each of the vector components of the electric field. Output from the sensors is fed into an amplifier (typically 25dB gain), and into a digital storage oscilloscope that sampled at a rate of 10Giga-sample/second.

Table 1. Experimental Conditions

SHOT#	V (km/s)	Target Thickness (mm)	Spacing (mm)	WP1 Thickness (mm)	Spacing (mm)	WP2 Thickness (mm)	Nitrogen Backfill (Torr)
OREX-1	6.0	Ti6Al4v/0.5	200	Al6061-T6/2.5	N/A	N/A	80
OREX-2	5.98	Ti6Al4v/0.5	200	Al6061-T6/2.5	N/A	N/A	80
OREX-3	5.973	Ti6Al4v/0.5	200	Al6061-T6/2.5	N/A	N/A	80
OREX-4	5.994	Ti6Al4v/0.5	200	OFHC Cu/4.85	N/A	N/A	80
OREX-5	6.059	Ti6Al4v/0.5	200	OFHC Cu/4.85	N/A	N/A	80
OREX-6	6.034	Ti6Al4v/0.5	200	Zn/3.17	N/A	N/A	80
OREX-7	6.036	Ti6Al4v/0.5	N/A	N/A	N/A	N/A	80
OREX-8	6.03	Ti6Al4v/0.5	200	Mg/0.5	N/A	N/A	.05
OREX-10	5.97	Ti6Al4v/0.5	N/A	N/A	N/A	N/A	.05
OREX-12	6.01	Ti6Al4v/0.5	40	In/0.5	40	Mg/0.5	.05
OREX-13	5.98	Ti6Al4v/0.5	40	In/0.5	40	In/1.0	.05
OREX-14	5.97	Ti6Al4v/0.5	N/A	N/A	N/A	N/A	.05
OREX-16	5.86	0.25 AL	40	In/0.5	40	Zn/0.5	.05
OREX-17	6.07	0.5 Mg	40	Al/0.5	40	In/0.5	.05

4. Results and analysis

In all experiments, target plates showed very clean cookie-cutter holes, approximately 3.05mm larger than the projectile diameter. Witness plates showed either small-diameter penetration holes or small-diameter spall bubble near the center of the plate, with multiple pits around the center. These plates size and material composition.were analyzed for statistics on debris

In the data reduction process, appropriate segments of data are selected (for each channel) to account for emissions from the target plate, and from each witness plate. Along with the data associated with each emission, an interval of several microseconds is also visually selected as being representative of background noise. As shown in Figure 2, the appropriate noise intervals are easily identified. The raw data are first corrected to account for the amplification gain. The corrected data, and corresponding noise records, are then transformed into the frequency domain using an FFT. The frequency domain output representation of both the background noise and the impact emission data are then corrected to account for the frequency dependent response of the E-field sensors. The Power Spectral Density (PSD) of the background noise is then subtracted from the PSD of the plate emission data. At this stage of the analysis, we have the frequency-domain representation of the electric field; the PSDs for each event are compared in the frequency domain. An inverse FFT provides the time-domain representation of the E-field.

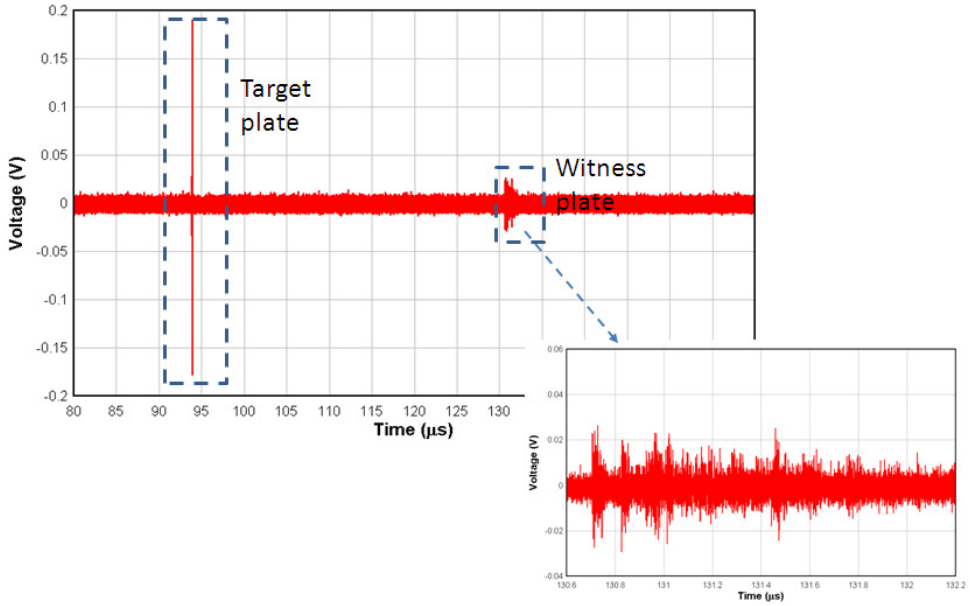

Fig 2. Typical output from impact event, showing emissions from target and witness plates.

Figure 2 shows a typical emission profile in the time-domain, including, an expanded view of the emissions from the witness plate; the individual pulses are several nanoseconds in duration . The characteristics of these emissions show the superposition of emissions from multiple impact events that are closely spaced in time. A significant part of our analysis attempted to develop an understanding of how this spectral detail is affected by impact velocity, material properties and material thickness.

RF data from all OREX experiments showed strong emissions from the target plate impacts, strong signals from the witness plate penetrations or spall bubbles, and multiple lower amplitude pulses consistent with impact pits around the central impact crater. These data were used to provide estimates of the relative magnitudes of the off-center impacts and time of occurrence of these events.

Several key features of the data are catalogued, as used a metrics to compare the responses of the various materials to similar impact conditions. We look at the duration of each pulse, the minimum amplitudes, the maximum amplitudes, and the dominant frequencies associated with each material. We also calculate the electromagnetic energy density associated with each pulse by integrating the electric fields of each of three perpendicular components:

$$U = \frac{1}{2}\frac{\epsilon_0}{\Delta t}\sum_{i=1}^{3}\int_{t1}^{t2} E_i^2(t)dt \qquad (1)$$

We find that energy density correlates closely with impact conditions and material thickness. Additionally, we find that the dominant frequency of emission correlates with the material, i.e. we see a unique spectral emission associated with each material that is impacted.

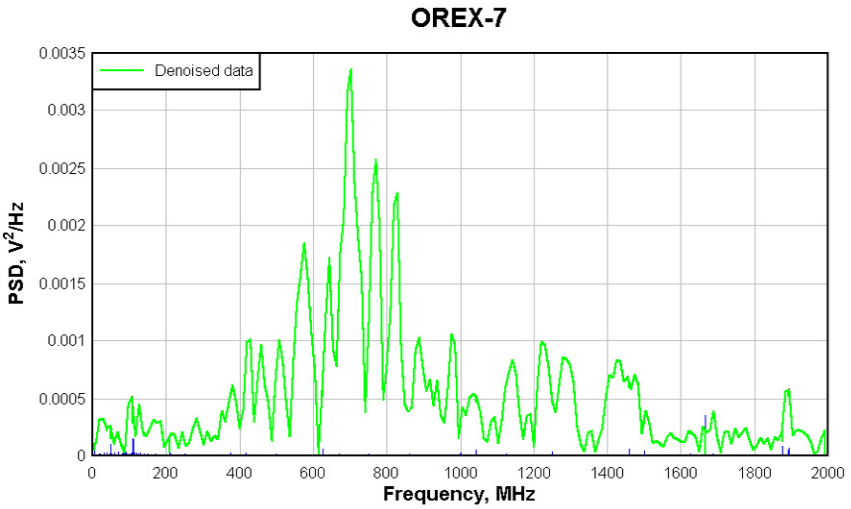

Fig.3. Typical frequency-domain emissions from hypervelocity plate impacts.

5. Summary and conclusions

Based on experience with emissions from explosively fractured metals, we have sought to determine if the results of the hypervelocity impact experiments are consistent with prior conclusions. We find that the basic concepts of the Misra Effect [7-10] in agreement with our data for this current series of measurements. Because of the multi-impact conditions of these experiments, it is difficult to correlate emission amplitude with impact damage. Nevertheless, our data show a unique spectral signature associated with each material. In an effort to identify the underlying physical processes responsible for these emissions, we have examined output from our computational models to understand the condition of the emitting materials. We conclude that during the several nanoseconds in which emissions occur, the material state within a small zone near the emitting surface is still in a solid-state, and is not yet in a melt phase. These results are consistent with prior work [2, 3] in which we have seen similar emissions at much lower impact velocities of approximately 1.5 km/s. We have examined the dependence of these effects on various material parameters, such as material strength, lattice spacing, Debye frequency and Debye temperature. Although we have not made an unequivocal determination of underlying mechanism, we see evidence of interesting correlations. For example, we see a relationship between the dominant frequency of emission and the Debye temperature, if we take lattice structure into consideration.

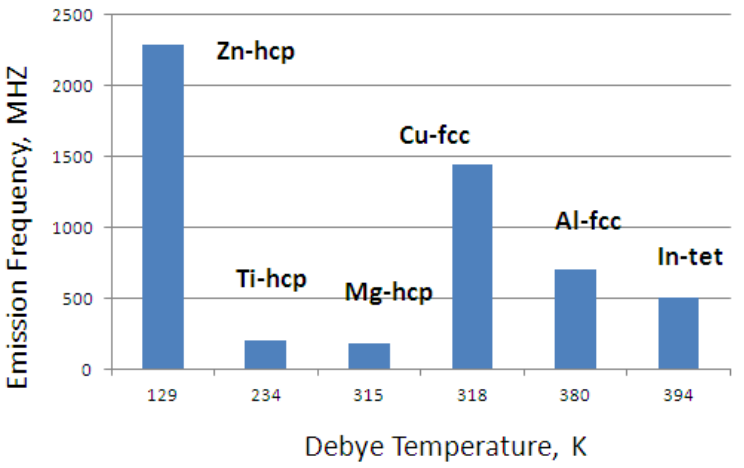

Fig. 4. Correlation between dominant frequency of emission and material strength.

Acknowledgements

Funding provided by the Missile Defense Agency under Contract HQ0147-10-C-0004.

References

[1] W. T. Brown, “Electromagnetic Emissions from Chemical Explosions: A Literature Review”, DTRA Report RT-2001-01-002 (SRF-151), November 2001.
[2] W. T. Brown, M. Schmidt and W. Broad, “Measurement and Analysis of Electromagnetic Emissions For the Divine Kingfisher-6 Event (Part 1 – Impact Phase)”, DTRA Report, March 15, 2006.
[3] W. T. Brown, M. Schmidt, P. Dzwilewski and T. Samaras, “Electromagnetic Radiation from the Detonation of Metal Encased Explosives,” In Shock Compression Of Condensed Matter -2001, American Institute Of Physics, 2005.
[4] W. Brown, M. Schmidt and W. Broad, “Measurement and Analysis of Electromagnetic Emissions for HUMBLE GINGKO Events”, Applied Research Associates Report ARA-T3-LR-1.21-13, November 2010.
[5] R. L. Moody and C. H. Conrad, “Magnetic induction system for two-stage gun projectile velocity measurements, ” Sandia National Laboratories Report No. SAND84-0638, May 1984.
[6] J. M. Mcglaun, S. L. Thompson and M. G. Elrick, “A Brief Description Of The Three-Dimensional Shock Wave Physics Code CTH,” ,” Sand89-0607, Sandia National Laboratories, Albuquerque, NM, 1989.
[7] A. Misra, “Electromagnetic Effects at Metallic Fracture“, Nature. 254, 133-134, 1975.
[8] A. Misra, R.C. Prasad, V. S. Chauham and R. Kumar, “**Effect of Peierls’ stress on the electromagnetic radiation during yielding of metals**”,
[9] Misra, A., Kumar, A., 2004, “Some aspects of electromagnetic radiation during crack propagation in metals”, Inter. J. of Fracture, 127(4):387-401.
[10] M. I. Molotskii, “Dislocation Mechanism for the Misra Effect”, Sov. Tech. Phys. Lett. 6(1), 22-23, 1980.
[11] G. Martelli and P. Cerroni, “On the theory of radio frequency emission from macroscopic hypervelocity impacts and rock fracturing,” Phys. Earth Planet. Inter.,40: 316-319.
[12] D. E. Grady and M. E. Kipp, “Geometric Statistics and Dynamic Fragmentation”, J. Appl. Phys., Vol. 58, 1210-1222, 1985.